

<https://doi.org/10.18524/1810-4215.2025.38.341473>

## REFLECTANCE SPECTRA OF DISTINCT SURFACE UNITS IN THE MARCIA CRATER REGION ON VESTA

V. V. Rychahova, I. G. Slyusarev

V. N. Karazin Kharkiv National University,  
Kharkiv, Ukraine, [richagova\\_valeriya@ukr.net](mailto:richagova_valeriya@ukr.net)

**ABSTRACT.** The pre-equatorial Marcia crater on asteroid (4) Vesta represents one of the youngest and best-preserved impact structures on the body, distinguished by its complex morphology and strong spectral variability. Within the Av-8 Marcia quadrangle, two spectrally and morphologically distinct surface units — pitted impact deposits (PIDs) and orange material patches (OMPs) — dominate the region and provide valuable insights into post-impact surface evolution. Using calibrated Framing Camera (FC) images from NASA's Dawn mission obtained during HAMO and LAMO phases, we analyzed the spectral characteristics of these units through color-ratio imaging ( $C(438 \text{ nm}/749 \text{ nm})$  and  $C(749 \text{ nm}/917 \text{ nm})$ ) and reflectance spectra derived from Level 1b datasets. Results show that both PIDs and OMPs display higher albedo, redder spectral slopes, and deeper  $0.9 \mu\text{m}$  pyroxene bands relative to surrounding materials, yet their spectral signatures differ markedly. PIDs generally exhibit deeper  $0.9 \mu\text{m}$  absorption bands and broader reflectance variability, while OMPs display consistently redder slopes and lower reflectance at 438 nm. Spatially, OMPs and PIDs frequently co-occur in the southwestern vicinity of Marcia crater, where lobate, flow-like morphologies also appear. Our findings confirm that simultaneous examination of  $C(438 \text{ nm}/749 \text{ nm})$  and  $C(749 \text{ nm}/917 \text{ nm})$  color-ratio maps is an effective approach to discriminate between OMPs and PIDs.

**Keywords:** asteroid (4) Vesta, reflectance spectra, color-ratio imagery, pitted impact deposits (PIDs), orange material patches (OMPs), flow-like features.

**АНОТАЦІЯ.** Кратер Марсія розташований у приекваторіальній частині астероїду (4) Веста та є однією з наймолодших і найкраще збережених ударних структур з виразною складною морфологією та значними спектральними варіаціями. У межах квадранту Av-8 Marcia переважають два морфологічно та спектрально відмінні типи поверхневих утворень — поклади ямчастих ударних структур (PIDs) та ділянки «помаранчевої» речовини (OMPs), які надають цінну інформацію про еволюцію поверхні після удару. Використовуючи відкалибровані зображення бортової камери Framing Camera (FC) місії NASA *Dawn*, отримані під час орбітальних фаз HAMO та LAMO, було проаналізовано за допомогою методу колориметричних відношень ( $C(438 \text{ nm}/749 \text{ nm})$  і  $C(749 \text{ nm}/917 \text{ nm})$ ) спектральні характеристики PIDs та OMPs. На основі відкалиброваних зображень Level 1b побудовано та

проаналізовано спектри відбивної здатності відповідних поверхневих утворень.

Результати показують, що як PIDs, так і OMPs характеризуються вищим альбедо, червонішим спектральним нахилом та глибшою смugoю поглинання піроксену на  $0.9 \mu\text{m}$  порівняно з навколошнім матеріалом, проте їх спектральні ознаки суттєво відрізняються порівняно одне з одним. PIDs, як правило, мають глибші смugi поглинання поблизу  $0.9 \mu\text{m}$  і більшу варіативність відбивної здатності, тоді як OMPs демонструють стабільно червоніший нахил спектра та нижчі значення відбиття на довжині хвилі  $438 \text{ nm}$ . Просторово обидва типи утворень часто спостерігаються разом у південно-західних околицях кратера Марсія, де також розташовані потокові структури.

Наши результати підтверджують, що одночасний аналіз карт колориметричних відношень  $C(438 \text{ nm}/749 \text{ nm})$  і  $C(749 \text{ nm}/917 \text{ nm})$  є ефективним методом для розрізнення OMPs та PIDs.

**Ключові слова:** астероїд (4) Веста, спектри відбивної здатності, метод колориметричних відношень, pitted impact deposits (PIDs), orange material patches (OMPs), потокові структури.

### 1. Introduction

Marcia crater located in equatorial part of asteroid (4) Vesta within Av-8 Marcia quadrangle and appears to be the youngest well-preserved crater on Vesta (Michalik et al., 2021). Crater's age is estimated by Williams et al. (2014) as 40 Ma (lunar-derived chronology model applied to the smooth part of elevated bench within southern crater floor) or 60 (asteroid flux-based chronology, smooth floor units) while ejecta blanket around Marcia is associated with older surface (120–150 Ma and 200–390 Ma as for lunar and asteroid flux-based chronologies, respectively). While majority of vestan craters is characterized by simple conical cavity, Marcia stands out by its complex morphology which manifests in presence of gully- and flow-like features, central peak, terraced rim and asymmetric shape of crater, being 58 km wide and 68 km long (Michalik et al., 2021). Along with morphological features, Marcia demonstrates non-uniform spectral (large variations of pyroxene band depths and reflectance) and thermal properties. Within the Av-8 quadrangle and Marcia Crater, two distinct surface units are of particular interest: pitted impact deposits (PIDs), notable for their characteristic morphology, and orange material patches (OMPs),

distinguished by their spectral properties. These units represent the primary focus of this study.

Pitted impact deposits (PIDs), previously known as *pitted terrains*, are (i) circular-shaped surface units with distinct pitted morphology and spectral behaviour as a rule demonstrating (ii) higher reflectance and (iii) deeper 0.9  $\mu\text{m}$  pyroxene band depth comparing to their immediate surroundings. This feature was found on a number of planetary bodies (Mars, Vesta, Ceres, Callisto, Europa, Mercury, Triton, Pluto) and related to the volatiles outgassing process (Michalik et al., 2021; Sizemore et al., 2017). The majority of PIDs population on Vesta (~96%) is located within Marcia crater and its vicinity, appearing as deposits within old altered craters' floors and/or depressions (Michalik et al., 2021). Within studied region PIDs are not homogenous in terms of spectral behavior and Michalik et al. (2021) outline two main types of PIDs based on differences in reflectance and mean  $C(749\text{nm}/917\text{nm})$  color ratio values, having Type 1 as units with higher reflectance and deeper 0.9  $\mu\text{m}$  band depths and Type 2 units exhibiting similar to background material values, although still preserving typical pitted morphology. Both types occur within and outside Marcia itself and belonging of each specific PID to one of two types is dependent on the hosting deposit's spectral properties (Michalik et al., 2021; Michalik et al., 2022). The additional feature of all PIDs is their redder slope comparing to immediate surrounding which makes these units distinct on the  $C(438\text{nm}/917\text{nm})$  color ratio distribution maps.

Orange material patches were previously known as light mantle, orange material lobate patches or 'pumpkin patches' as one of three types of orange material deposits (along with diffuse dark mantle ejecta and ejecta rays from young fresh-looking craters). Orange material takes its name after its orange-to-red tones on the global false-colour mosaics in Clementine colours ( $R=C(750\text{nm}/450\text{nm})$ ,  $G=C(750\text{nm}/920\text{nm})$ ,  $B=C(450\text{nm}/750\text{nm})$ ) (LeCorre et al., 2013; Garry et al., 2014) and was interpreted as an impact melt with possible cumulative eucrite component (LeCorre et al., 2013). In this study we suggest to name such deposits as orange material patches (OMPs) regarding their irregular shapes and redder spectral slope. OMP is a widespread surface unit which covers almost whole asteroid's equatorial belt excluding relatively narrow range of longitudes (from 30°E to 90°E with several rare occurrences of separate OMPs). Shapes and sizes of OMPs strongly vary with their location along Vesta's surface – from single spots with diameter of around 0.7 km to 60-km long assemblage of patches, having roundish to fully irregular outlines. As mentioned above, the spectral behavior of OMPs is generally characterized by a redder spectral slope — presumably due to an absorption feature near 438 nm (Rychahova et al., 2024) — as well as by higher overall reflectance and, typically, deeper 0.9  $\mu\text{m}$  pyroxene absorption bands compared to the surrounding material. Nevertheless, global population of OMPs appears to be quite non-homogeneous demonstrating a high level of diversity of edge sharpness, sizes, and variations of absorption at 438 nm within a single spot (Rychahova et al., 2024).

OMPs and PIDs have a number of common features (higher albedo, steeper slope of spectra, deeper 0.9  $\mu\text{m}$  pyroxene band) while still demonstrating differences in morphology, size distribution and diversity of shapes. Their

close location within Av-8 quadrangle makes this region an interception of two distinct surface units gives an opportunity to compare spectral characteristics of OMPs and PIDs in case of close disposition and identical surroundings. Additionally, vicinity of Marcia demonstrates presence of lobate and flow-like features related to the impact melt originated during Marcia (and possibly Calpurnia) formation (Williams et al., 2014). These flows occasionally demonstrate various pitted morphology and appear to be of high interest along with OMPs and PIDs population. In this study, we focus primarily on comparing the spectral properties of OMPs and PIDs, including several samples associated with a flow-like feature near the southern rim of Marcia crater.

## 2. Methods and data

We used Level 1b calibrated images obtained by NASA Dawn's spacecraft on-board imager Framing Camera (FC) during HAMO and LAMO orbital mapping phases (spatial resolution 62 m/pxl and 20 m/pxl, respectively). The Framing Camera (FC) instrument was equipped with one clear filter (F1) and seven narrow bandpass filters (F2–F8), covering the visible to near-infrared wavelength range (from 438 nm for F8 to 965 nm for F2) and make it possible to apply color-ratio imagery technique in order to analyze spectral characteristics of selected surface units.

The data used in this study are available in free access as a part of Planetary Data System archive (<https://sbn.psi.edu/pds/sbib/>). All coordinates provided in Claudia coordinate system, which is the main preferable coordinate system.

Color-ratio imagery was initially invented as an approach to examine and analyze spectral behavior of selected areas on lunar surface and required at least two to pixel-by-pixel coaligned images obtained at close phase angle values and different wavelengths  $\lambda_1$  and  $\lambda_2$  (Kaydash et al., 2010). After spectral calibration and alignment procedure were preformed, images can be divided by each giving the output which represents a map of color ratio  $C(\lambda_1/\lambda_2)$  distribution along the studied area. Obtained color-ratio distribution map gives an opportunity to identify spectrally distinct surface units such as young craters ejecta halo, taluses, indications of impact melt presence, etc. Simultaneous analysis of color-ratio distribution maps corresponding to different spectral characteristics (slope of spectra, band depth, spectral bend at specific wavelength, etc.) and reflectance images allows accurate classification of distinct spectral units and contributes to the interpretation of their formation processes. In this study we built color ratios  $C(438\text{nm}/749\text{nm})$  and  $C(749\text{nm}/917\text{nm})$  distribution maps of selected regions within Marcia crater and its vicinity. The color ratio  $C(438\text{nm}/749\text{nm})$  is used to discriminate areas with differing spectral slopes. Regions exhibiting lower ratio values (appearing as darker tones on the map) represent one of our key indicators used to identify OMP units. In contrast, the color ratio  $C(749\text{nm}/917\text{nm})$  is sensitive to the depth of the 0.9  $\mu\text{m}$  pyroxene absorption band, and higher ratio values correspond to areas characterized by a deeper band.

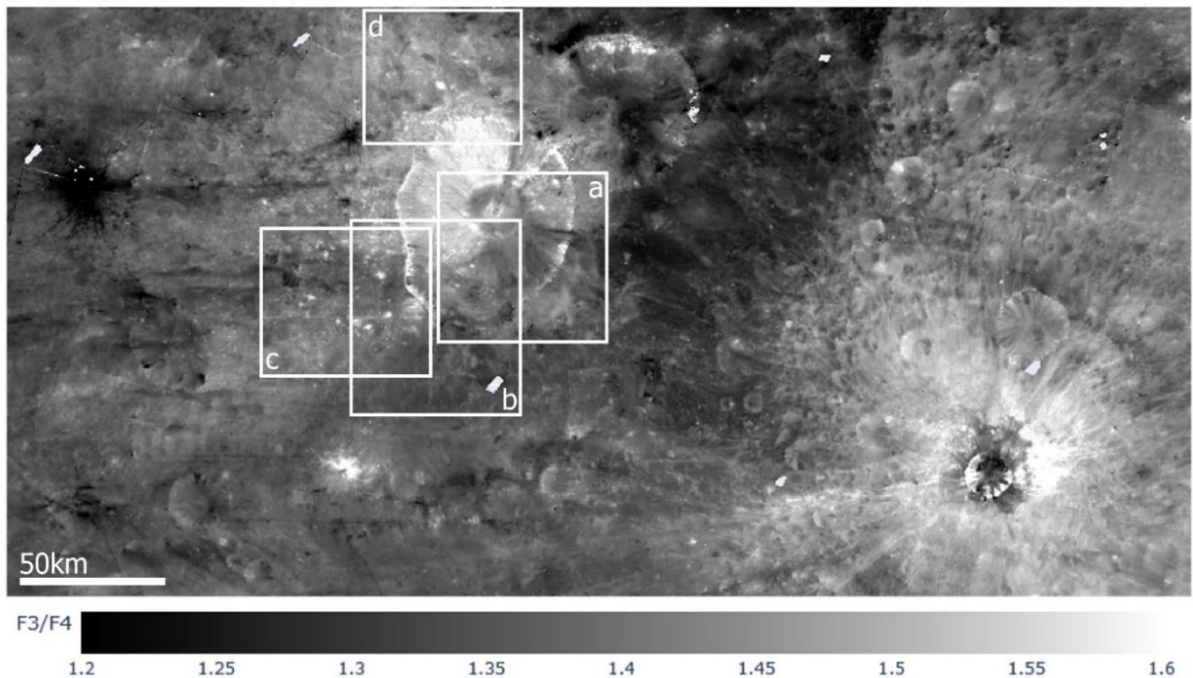


Figure 1: Color ratio  $C(438\text{nm}/749\text{nm})$  distribution map of Marcia crater region. White boxes a—d define specific areas which were selected for detailed analysis.

### 3. Results

We selected 4 images series (regions a—d, Fig.1) within Marcia crater vicinity and crater's floor in order to build color ratio distribution maps  $C(438\text{nm}/749\text{nm})$ ,  $C(749\text{nm}/917\text{nm})$  and normalized reflectance spectra for 15 PIDs (6 outside Marcia and 9 within crater's floor) and 10 OMPs.

#### 3.1. Spatial distribution

As OMPs and PIDs are distributed unequally along the region, we focused our attention on the areas which contain mostly both PIDs and OMPs simultaneously. The highest concentration of co-occurring units is observed in the region between the southwestern rim of Marcia crater and Eumachia crater (Fig.1c). Seven of ten studied OMPs and four PIDs placed within the region, including cases of OMPs and PIDs close occurrences (Table 1, b and d). Region b (SW rim of Marcia crater and southern crater's vicinity) partially includes samples from the region c as well as PIDs within Marcia's terrace and flow-like features near the crater rim. Region d is not abundant with prominent occurrences of both units and counts just one remarkable PID and 3 relatively small OMPs. We do not observe OMPs within Marcia's terrace and floor which are covered by region a. We do not include the full list of all units present within the region, but focus on the most prominent example which is available for morphologic and spectral analyses as representatives of each group. Along with typical PIDs there's a number of cases of pitted surface within flow-like lobate features within the southern and eastern vicinity of Marcia rim. Those PIDs vary in terms of shapes and sizes (from irregular roundish clusters of pits to elongated wide stripes

that align with the lobate feature), as well as in spectral characteristics. Due to the ambiguity in defining the boundaries of individual PIDs and the limitations in obtaining reliable spectra for some of them, these cases were excluded from our analysis.

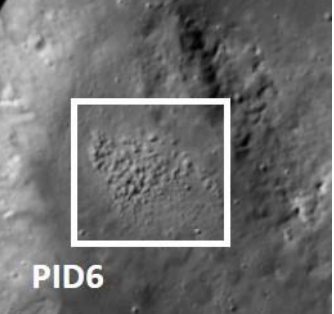
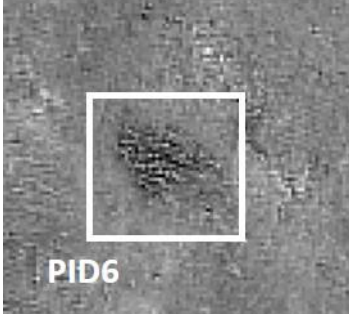
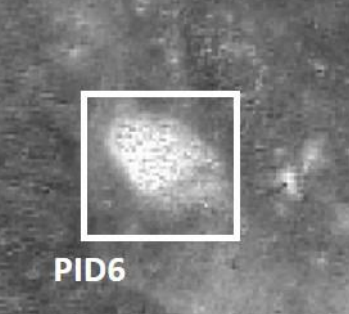
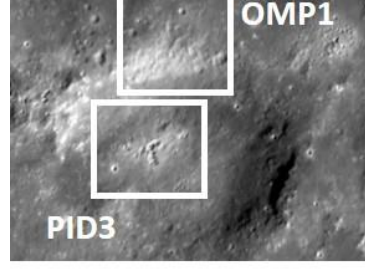
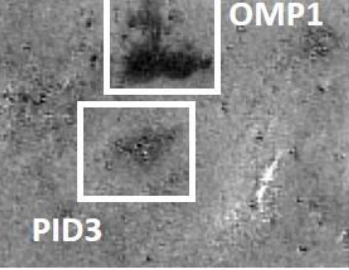
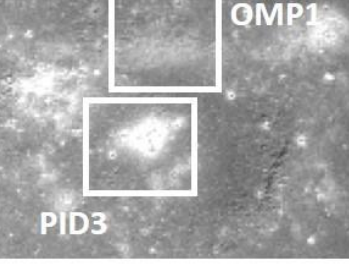
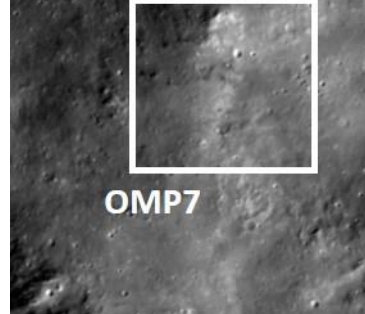
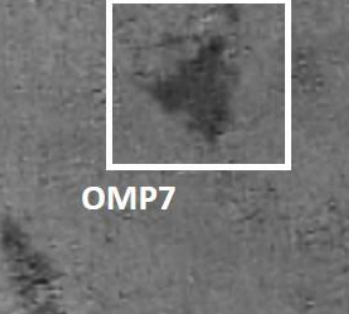
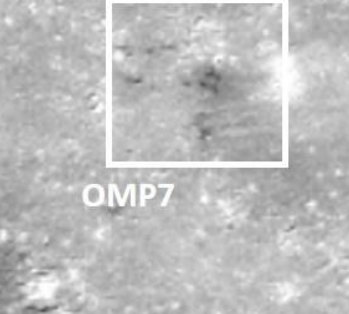
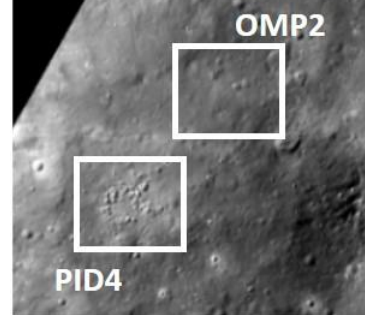
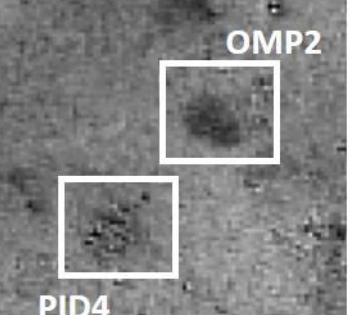
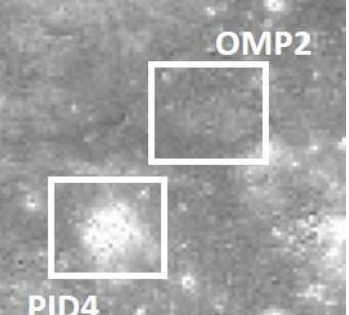
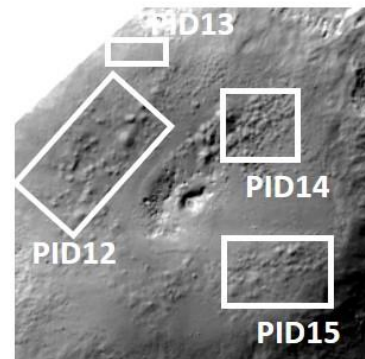
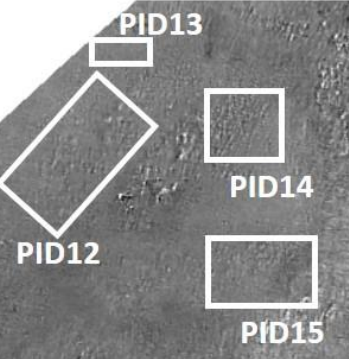
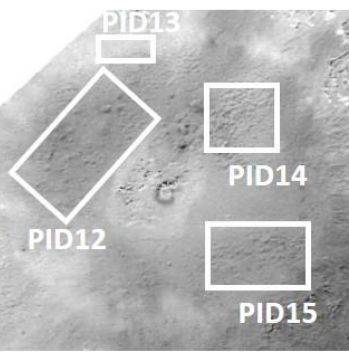
#### 3.2. Sizes and shapes

Within our sample, the large part of units of both types exhibits roundish shapes with mean diameter around 2–3 km, while irregular-shaped deposits also occur within OMPs type more frequently. Presence of such complex shapes of OMPs clusters (e.g., OMP assemblages which bear OMP4–6) makes it more difficult to establish accurate upper bound for size. While in general OMPs' upper bound is much larger (up to 60 km), within Marcia crater region the maximal size of OMPs assemblage is around 5–6 km comparing to the largest PIDs cluster with size of 11.36 km (PID12). The mean value is slightly greater for PIDs due to presence of large cluster within crater floor (PIDs: 3.06 km; OMPs: 2.88 km). Minimum values are similar for both unit types – 0.68 km and 0.78 km (OMPs and PIDs, respectively).

#### 3.3. Spectral behavior

For all selected PID and OMP samples, reflectance and normalized reflectance spectra were produced. The general spectral characteristics, including variations in spectral slope and the  $0.9\text{ }\mu\text{m}$  pyroxene band depth, are summarized in Fig.2. Two reference spectra were selected to facilitate quantitative comparison between the spectra of distinct surface units: (a) background material sample within Marcia region which does not differ from the majority of surface by reflectance or values of  $C(438\text{nm}/749\text{nm})$  and  $C(749\text{nm}/917\text{nm})$ ;

Table 1: Comparison of morphological settings and color ratio distribution maps

	Morphological settings	C(438nm/749nm)	C(749nm/917nm)
a	 PID6	 PID6	 PID6
b	 OMP1 PID3	 PID3	 OMP1 PID3
c	 OMP7	 OMP7	 OMP7
d	 OMP2 PID4	 PID4	 OMP2 PID4
e	 PID12 PID13 PID14 PID15	 PID12 PID13 PID14 PID15	 PID12 PID13 PID14 PID15

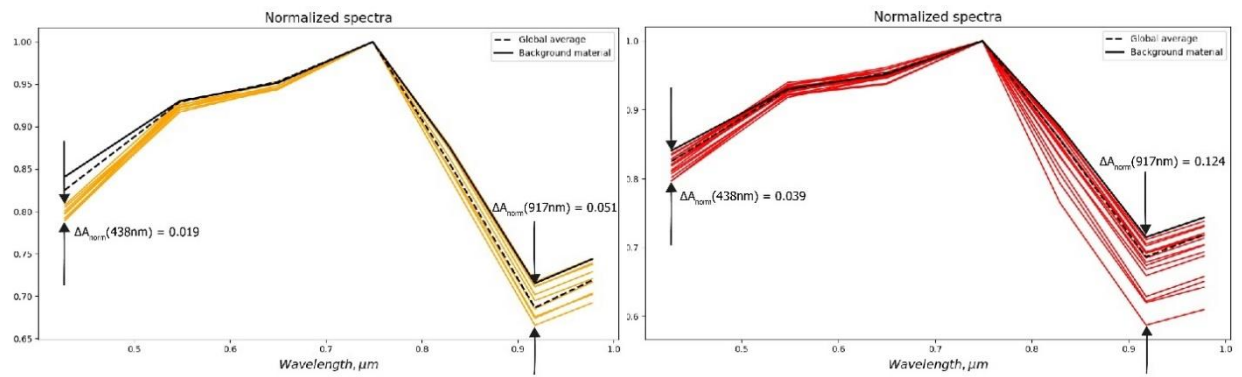
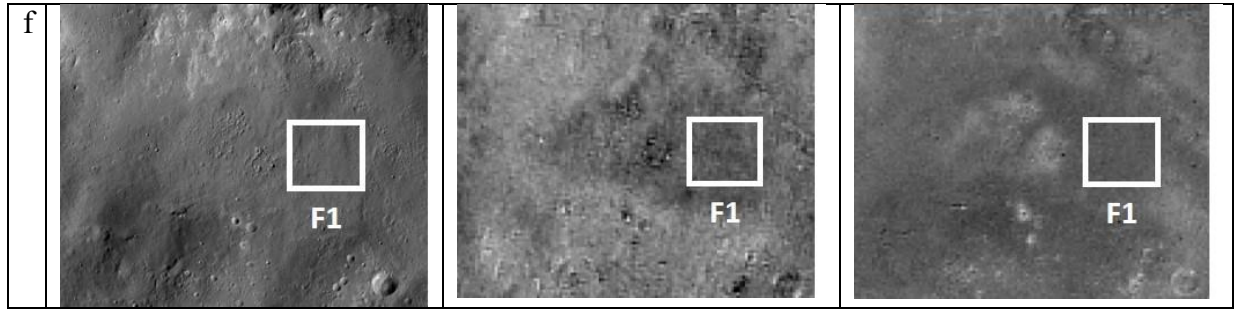


Figure 2: Normalized reflectance spectra for selected units with comparison of values variance at 438 nm and 917nm. Left panel – OMPs. Right panel – PIDs.

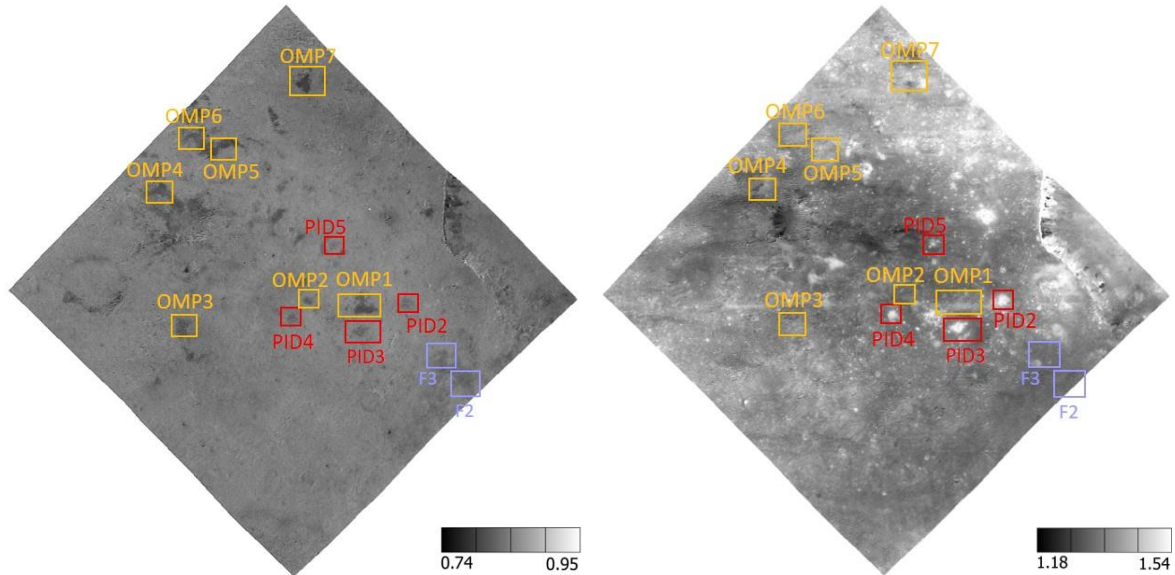


Figure 3: Color-ratio distribution maps of region c (Fig. 1). Left panel –  $C(438\text{nm}/749\text{nm})$ , lower values correspond to redder spectral slopes. Right panel –  $C(749\text{nm}/917\text{nm})$ , lower values correspond to not shallower 0.9  $\mu\text{m}$  pyroxene bands.

Table 2: Catalogue of selected surface units (PIPs, OMPs, flow-like features)

Name	Coordinates	Size, km	C(438nm/749nm)	C(749nm/917nm)	A(750 nm)
OMP1	181.24 °E, 2.05 °N	.33	0.81	1.40	0.19
OMP2	179.51 °E, 2.26 °N	1.74	0.82	1.35	0.17
OMP3	175.52 °E, 1.4 °N	3.26	0.82	1.37	0.17
OMP4	174.82 °E, 5.88 °N	3.10 (5.15 long x 4.47 wide)	0.81	1.36	0.17
OMP5	176.87 °E, 7.33 °N	4.62 (6.35 long)	0.81	1.43	0.19
OMP6	176.28 °E, 7.12 °N	3.78 (6.35 long)	0.82	1.41	0.18
OMP7	179.35 °E, 9.28 °N	2.88	0.79	1.43	0.18
OMP8	179.03 °E, 19.41 °N	0.68	0.80	1.55	0.19
OMP9	179.57 °E, 19.14 °N	1.36	0.79	1.56	0.19
OMP10	183.07 °E, 18.12 °N	4.09	0.81	1.49	0.18
PID1	181.24 °E, 2.05 °N	3.01	0.84	1.36	.15
PID2	180.0 °E, 2.21 °N	1.56	0.85	1.5	0.17
PID3	181.19 °E, 1.24 °N	1.45	0.84	1.52	0.20
PID4	178.98 °E, 1.73 °N	1.00	0.84	1.51	0.19
PID5	180.32 °E, 4.04 °N	0.78	0.85	1.44	0.18
PID6	186.31 °E, 18.66 °N	3.23	0.81	1.68	0.20
PID7	189.06 °E, 1.78 °N	2.23	0.81		0.16
PID8	187.55 °E, 1.56 °N	3.45	0.79	1.33	0.15
PID9	187.12 °E, 2.32 °N	1.23	0.81	1.30	0.15
PID10	186.52 °E, 2.43 °N	1.67	0.83	1.34	0.17
PID11	186.09 °E, 3.07 °N	1.23	0.83	1.37	0.17
PID12	190.84 °E, 10.57 °N	11.36	0.84	1.32	0.17
P I	189.22 °E, 11.43 °N	3.23 (the whole circle – 59.13)	0.84	1.49	0.20
P I	191.7 °E, 10.57 °N	4.90	0.84	1.37	0.18
PID15	191.49 °E, 8.74 °N	5.79	0.84	1.32	0.17
F1	186.52 °E, 0.16 °N	4.16	0.84	1.28	0.16
F2	184.37 °E, 0.0 °S	2.27	0.84	1.30	0.16
F3	183.83 °E, 0.49 °N	3.40	0.85	1.31	0.17

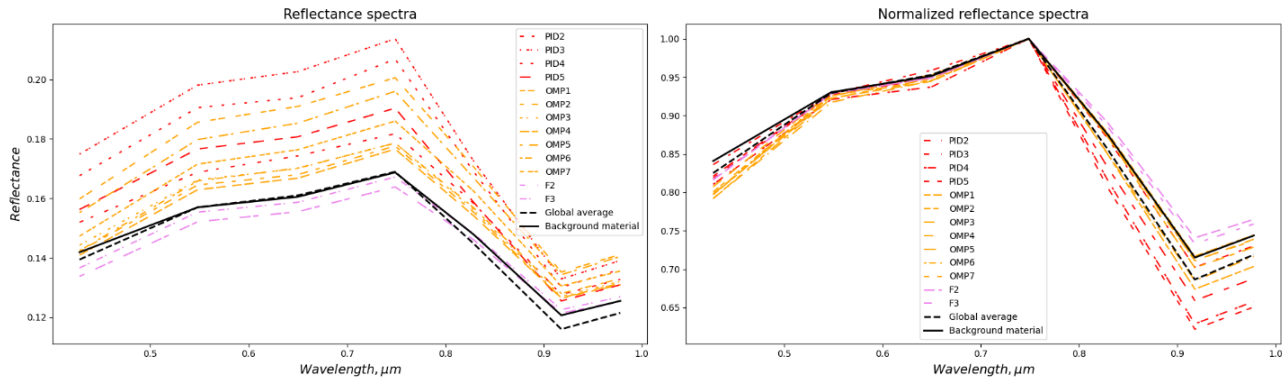


Figure 4: Reflectance (a) and normalized (b) reflectance spectra of units within region c (Fig. 1)

(b) global average spectra of the vestan surface. While PIDs and OMPs demonstrate similar characteristics comparing to background material – lower reflectance at 438 nm (redder spectral slope) and deeper pyroxene band at 0.9  $\mu\text{m}$ , – the spectral behavior of units comparing to each other slightly differs. We can observe tendency to lower reflectance values at 438 nm and shallower band depths for OMPs comparing to PIDs. Additionally, OMPs demonstrate lower degree of variance of above the mentioned characteristics, especially for values of normalized reflectance at 917 nm which is associated with position of pyroxene band center (Fig. 2).

Average global vestan spectra show distinct behavior comparing to typical background material in Marcia region with redder slope between 438 nm and 555 nm and higher values of pyroxene band depth. According to this, OMP units still demonstrate redder slope in comparison to average spectra, while a number of PIDs doesn't follow this rule anymore. In terms of band depths, both unit types include several samples with shallower than average bands, but majority of PIDs still demonstrate higher band depths values.

Distributions of reflectance spectra at maximum wavelength (749 nm) point that PIDs in general tend to have slightly wider range of values than OMPs (Table 2, PIDs: 0.15–0.20; OMPs: 0.17–0.19). Color ratio  $C(749\text{nm}/917\text{nm})$  and  $C(438\text{nm}/749\text{nm})$  distribution maps provides a spatial context of how PIDs and OMPs behave along the region (Fig.3). Lower values (dark tones) on  $C(438\text{nm}/749\text{nm})$  map characterize surface as such with a redder slope (lower reflectance at 438 nm) and the most prominent feature on these maps are OMPs, while PIDs differ from background material but at the much lower degree. The opposite situation is present on the  $C(749\text{nm}/917\text{nm})$  map, where PIDs along with ejecta from small young craters demonstrate the highest values of color ratio and deeper pyroxene band, respectively. These facts confirm our results derived from comparison of normalized reflectance spectra of both unit types.

Additionally, comparison of the normalized reflectance spectra of both unit types with flow-like features indicates that this material exhibits an intermediate spectral slope between PIDs and OMPs, while the depth of the 0.9  $\mu\text{m}$  band is significantly shallower than that of the background material and the global average spectrum of Vesta.

#### 4. Conclusion

As known from previous studies, both OMPs and PIDs exhibit irregular shapes, however distinctive morphology features are only associated with PIDs. We found that PIDs have much smaller characteristic sizes than OMPs on a global scale, although they exhibit larger mean sizes within the studied region, particularly for PIDs on the Marcia crater floor. In terms of spatial distribution, PIDs are associated with a few craters (the Marcia region hosts ~96% of all PIDs on Vesta), while OMPs are widespread with gap on 30°E – 90°E.

Analysis of PIDs and OMPs spectra show that in comparison with typical surrounding material OMP and PID have slightly higher apparent albedo, deeper 0.9  $\mu\text{m}$  pyroxene band and lower values of reflectance at 438 nm, however both surface units show prominent differences in spectral behavior comparing to each other. Namely: (a) OMPs always show lower reflectance at 438 nm in comparison with PIDs; (b) PIDs demonstrate significantly deeper pyroxene band depth in comparison with OMP. Additionally to the previously mentioned differences, we found out that the best way to distinguish OMPs and PIDs is simultaneous analysis of  $C(438\text{nm}/749\text{nm})$  and  $C(749\text{nm}/917\text{nm})$  color ratio distribution maps.

Flow-like features have lower reflectance at 438 nm in comparison with average vestan surface. Areas where flow-like features host PIDs material show deeper pyroxene band comparing to the rest of flow-like features.

#### References

- Garry W.B. et al.: 2014, *Icar*, **244**, 104.
- Kaydash V. et al.: 2010, *SoSyR*, **44**, 267.
- Le Corre L. et al.: 2013, *Icar*, **226**, 1568.
- Michalik T. et al.: 2021, *Icar*, **369**, 114633.
- Michalik T. et al.: 2022, *PSJ*, **3**, 182.
- Rychahova V. et al.: 2024, EPSC2024-577.
- Sizemore H. G. et al.: 2017, *GeoRL*, **44**, 6570.
- Williams D. A. et al.: 2014, *Icar*, **244**, 74.
- Williams D. A. et al.: 2014, *P&SS*, **103**, 24.